Proteolytic cleavage of the extracellular domain affects signaling of parathyroid hormone receptor 1

1 **Christoph Klenk[1,#*], Leif Hommers[2,3,4], Martin Lohse[1,5,6,7]**

2 [1]Institute of Pharmacology and Toxicology, University of Würzburg, Würzburg, Germany
3 [2]Interdisciplinary Center for Clinical Research, University Hospital of Würzburg, Würzburg,
4 Germany
5 [3]Department of Psychiatry, Psychosomatics and Psychotherapy, Center for Mental Health,
6 University Hospital of Würzburg, Würzburg, Germany.
7 [4]Comprehensive Heart Failure Center (CHFC), University Hospital of Würzburg, Würzburg,
8 Germany.
9 [5]Rudolf Virchow Center, University of Würzburg, Würzburg, Germany
10 [6]Max Delbrück Center for Molecular Medicine (MDC), Berlin, Germany
11 [7]ISAR Bioscience Institute, Planegg, Germany
12 [#]present address: Department of Biochemistry, University of Zurich, Zurich, Switzerland
13

14 * Corresponding author: Christoph Klenk, c.klenk@bioc.uzh.ch
15

Abstract

Parathyroid hormone 1 receptor (PTH1R) is a member of the class B family of G protein-coupled receptors, which are characterized by a large extracellular domain required for ligand binding. We have previously shown that the extracellular domain of PTH1R is subject to metalloproteinase cleavage *in vivo* that is regulated by ligand-induced receptor trafficking and leads to impaired stability of PTH1R. In this work, we localize the cleavage site in the first loop of the extracellular domain using amino-terminal protein sequencing of purified receptor and by mutagenesis studies. We further show, that a receptor mutant not susceptible to proteolytic cleavage exhibits reduced signaling to G_s and increased activation of $G_{q/11}$ compared to wild-type PTH1R. These findings indicate that the extracellular domain modulates PTH1R signaling specificity.

Introduction

Parathyroid hormone receptor 1 (PTH1R) is a key regulator of blood calcium levels and bone metabolism in response to parathyroid hormone (PTH). Moreover, activation of PTH1R by parathyroid-related hormone peptide (PTHrP) has been implicated in fetal development and in malignancy-associated hypercalcemia (1). PTH1R is a member of the class B family of G protein-coupled receptors (GPCRs) which are characterized by a large N-terminal extracellular domain (ECD; ~100 to 180 residues) that is critically involved in ligand binding (2,3). Similar to other class B GPCRs, the ECD of PTH1R consists of two pairs of antiparallel β-strands flanked by a long and a short α-helical segment at the N- and C-terminal end, respectively. The overall conformation is constrained by three conserved disulfide bonds which are required for proper folding and for ligand binding (4-7). The ECD is oriented in an upright position above the membrane surface with residues 15-34 of PTH binding into a groove formed by the ECD and the N-terminal part of the ligand protruding as a continuous α-helix into the transmembrane domain of PTH1R (7) (Fig. 1). In line with the receptor structure, a two-step activation model has been proposed, where first the C-terminal part of PTH binds to the extracellular domain, and then the N-terminal part of PTH interacts with the receptor core, thereby leading to receptor activation (8,9). PTH1R couples to multiple heterotrimeric G protein subtypes and can activate several signaling pathways concomitantly. Predominantly, adenylyl cyclases are stimulated by activation of G_s as well as phospholipase Cβ by G_q (10-12). Moreover, activation of $G_{i/o}$ resulting in inhibition of adenylyl cyclase and activation of $G_{12/13}$ leading to phospholipase D and RhoA activation, as well as activation of mitogen-activated protein kinases through G protein-dependent and -independent mechanisms

have been reported (13-18). PTH1R activation can have anabolic and catabolic effects on bone. While continuous administration of PTH enhances osteoclastogenesis leading to bone resorption and calcium liberation, intermittent administration of PTH results in bone formation through enhancing osteoblast differentiation and survival, which is used as a treatment option for severe osteoporosis (19,20). Although the exact molecular mechanisms are not clear yet, differential activation of signaling pathways seems to play an important role in these opposing effects upon PTH1R activation. While G_s-signaling is the predominant pathway for promoting PTH-induced bone formation, G_q-activation seems to have little or no effect on osteogenesis (21-23). In addition, β-arrestin recruitment was shown to be essential for selectively promoting bone formation upon treatment of mice with recombinant PTH(1-34) (24). Moreover, many of these effects appear to be regulated in a tissue- and cell-type specific manner (25).

We have previously shown that the ECD of PTH1R can undergo proteolytic cleavage by an extracellular metalloproteinase resulting in reduced stability and degradation of the receptor. We also demonstrated that N-terminal ECD cleavage occurred only at the cell surface, and that internalization of the receptor resulting from continuous activation by agonists prevented cleavage and thereby stabilized the receptor. Furthermore, our experiments suggested that the cleavage site is located within the first 90 residues of the receptor, however the exact position was not fully resolved (26). In the present study, we have localized the cleavage site in the unstructured loop of exon E2 within the PTH1R ECD. Moreover, we demonstrate that ECD cleavage results in an altered ligand efficacy of PTH changing the G protein-coupling of PTH1R from G_q to G_s.

Materials and Methods

Materials

Lipofectamine 2000 was purchased from Invitrogen. [$Nle^{8,18}$,Tyr^{34}]PTH (1-34), referred to as PTH(1-34) was purchased from Bachem. Generation of a polyclonal rabbit anti-PTH1R (1781) antiserum was described previously (27). Anti-rabbit peroxidase-conjugated secondary antibodies were obtained from Dianova. Cy2-conjugated anti-mouse antibody was from Jackson Immuno Research Lab. EXPRE [^{35}S] protein labeling mix was from Perkin Elmer. All cell culture media were obtained from PAN Biotech. All other reagents were from Sigma-Aldrich or Applichem.

81 **cDNA constructs**

82 A Strep-Tag II (WSHPQFEK) was fused to the C-terminal end of human PTH1R (26) by
83 PCR. Alanine mutations were introduced into the extracellular domain of PTH1R by overlap
84 extension PCR. In total, 6 constructs with alanine blocks from Leu^{56}-Met^{63}, Glu^{64}-Ser^{71},
85 Ala^{72}-Arg^{79}, Lys^{80}-Leu^{87}, Tyr^{88}-Lys^{95}, and Glu^{96}-Tyr^{103} were generated. All constructs were
86 subcloned into pcDNA5/FRT vector (Thermo Fisher Scientific) using the restriction sites
87 EcoRI and ApaI and verified by sequencing.

88 **Cell culture and transfection**

89 Flp-In CHO cells (Thermo Fisher Scientific) were maintained in 1:1 Dulbecco's modified
90 Eagle's medium/ Ham's F12 medium containing 10 % (v/v) fetal calf serum, 100 U/ml
91 penicillin, 100 µg/ml streptomycin and 100 µg/ml Zeocin (Thermo Fisher Scientific). Cells
92 were maintained at 37 °C in a humidified atmosphere of 5% CO_2, 95% air. To generate stable
93 cell lines, cells were transfected with pcDNA5/FRT-PTH1R plasmids using Lipofectamine
94 2000 according to the manufacturer's instructions. 48 h after transfection, cells were selected
95 in culture medium where Zeocin was replaced by 600 µg/ml hygromycin B for approximately
96 two weeks. Clonal cell lines were derived from limited dilution series and screened for
97 expression of PTH1R by Western blot and immunocytochemistry.

98 **SDS-PAGE and Western blotting**

99 Cells were lysed in SDS-loading buffer (50 mM Tris [pH 6.8], 2% (v/v) SDS, 10% glycerol, 5
100 mg/ml bromophenol blue) for 20 min on ice, briefly sonified and incubated at 45 °C for 20
101 min. For reducing conditions, 4% (v/v) β-mercaptoethanol was added to the lysis buffer.
102 Lysates were cleared by centrifugation and run on 10% SDS-polyacrylamide gels in a Mini-
103 PROTEAN 3 cell apparatus (Biorad). Proteins were electroblotted onto Immobilon P
104 membranes (Millipore) using a Bio-Rad Mini trans-blot cell apparatus at 100 V for 60 min at
105 4 °C. The blots were probed with anti-PTH1R antibodies (1:4000), followed by horseradish
106 peroxidase-conjugated goat anti-rabbit (1:10000) and detection on Super RX X-ray film
107 (Fujifilm) using ECL Plus reagent (GE Healthcare).

108 **Purification of PTH1R**

109 Membranes from Flp-In CHO cells stably expressing PTH1R-Strep2 were prepared as
110 described before (28). Membranes were solubilized in solubilization buffer (50 mM Tris-HCl,
111 pH 7.4, 140 mM NaCl, 0.5% (w/v) n-dodecyl β-D-maltoside, 10 µg/ml soybean trypsin
112 inhibitor, 30 µg/ml benzamidine, 5 µg/ml leupeptin, 100 µM PMSF) for 2 h, and insoluble
113 material was removed by centrifugation for 1 h at 100,000 × g. Solubilized PTH1R-Strep2

114 was incubated with 1 ml Strep-Tactin sepharose (IBA GmbH) for 12 h under constant
115 agitation and washed with 10 column volumes of wash buffer (100 mM Tris-HCl [pH 8.0],
116 1 mM EDTA, 150 mM NaCl, 0.1% (w/v) n-dodecyl β-D-maltoside). Bound receptor was
117 eluted with 1-2 column volumes of the same buffer supplemented with 2.5 mM desthiobiotin
118 and concentrated with a Microcon centrifugal filter device (10,000 MWCO, Millipore).

119 **Amino-terminal sequencing of cleaved receptor fragments**

120 Fifty µg of purified receptor fragments were blotted onto PVDF membranes and stained with
121 Coomassie Blue. The fragments were excised and subjected to automated Edman degradation
122 (Wita GmbH).

123 **Immunocytochemistry and confocal imaging**

124 CHO cells stably expressing PTHR variants were grown on coverslips overnight. Cells were
125 then exposed (or not) to 100 nM PTH(1-34) for 30 min as indicated. Cells were fixed with 4%
126 paraformaldehyde and 0.2% picric acid in 0.1 M phosphate buffer, pH 6.9, for 30 min at room
127 temperature and washed five times in PBS. For permeabilization cells were incubated for
128 5 min in methanol. After 10 min of preincubation in PBS containing 0.35% BSA, cells were
129 incubated with anti-PTH1R antibody at a dilution of 1:2000 in PBS containing 0.35% BSA
130 for 1 h at 37 °C. Bound primary antibody was detected with Cy2-labeled goat anti-rabbit IgG
131 (1:400). Specimens were examined using a Leica SP2 laser scanning confocal microscope.

132 **Functional receptor assays**

133 Signaling assays were measured in Flp-In CHO cells stably expressing the indicated PTH1R
134 variants. cAMP was measured using a RIA kit (Beckman Coulter) and inositol phosphates
135 were separated by chromatographic separation of [myo-2-^{3}H]inositol phosphates as described
136 previously (29).

137 Results

138 Our previous findings suggested that the protease cleavage site is most likely located between
139 Cys^{48} and Cys^{108} (26), a region including exon E2 of PTH1R which is unique among all other
140 class B GPCRs and which forms a disordered loop in the crystal structures of the isolated
141 PTH1R ECD (4) and full length PTH1R (7) (Fig. 1). We therefore created a series of mutants
142 where stretches of 8 residues in this region were mutated to Ala to delineate the protease
143 cleavage site (Fig. 2A). Each of the six resulting PTH1R variants was stably expressed in
144 Flp-In CHO cells, and expression and membrane targeting of the receptor were analyzed by
145 immunofluorescence (Fig. 2B) using an antibody detecting the C-terminal part of PTH1R

146 (26,27). All mutants exhibited a distinct membrane staining which was comparable to that of
147 wild-type receptor. Upon stimulation with 100 nM PTH(1-34) for 30 min, a sequestration of
148 receptor from the cell surface into endocytic vesicles was observed suggesting that each
149 receptor variant activated intracellular signaling pathways leading to receptor internalization.
150 To test whether any of the mutations had an effect on protease cleavage, the migration
151 patterns of PTH1R variants were analyzed by reducing SDS-PAGE and Western blotting. As
152 demonstrated previously, after extracellular protease cleavage the N-terminal part of the ECD
153 (~10 kDa) remains tethered to the receptor core by a single disulfide bond but was lost under
154 reducing conditions leading to an apparent molecular weight of the receptor of ~80 kDa (26).
155 In contrast, sustained receptor activation by PTH(1-34) resulting in continuous receptor
156 internalization rendered the receptor inaccessible for extracellular proteases and thus
157 protected the full-length receptor with a molecular weight of ~90 kDa (Fig 2C, left panel; c.f.
158 (26)). Mutants where residues 64-71, 80-87, 88-95 or 96-103 had been replaced by alanines
159 migrated at ~80 kDa in reducing SDS-PAGE, indicating that protease cleavage was not
160 prevented by the respective mutations. In contrast, $PTH1R^{56-63A}$ exclusively migrated at ~90
161 kDa similar to the non-cleaved wild-type receptor. For $PTH1R^{72-79A}$ two bands were detected
162 which co-migrated with the cleaved and non-cleaved receptor species. Thus, mutating the
163 region between Leu^{56} and Met^{63} to alanine fully inhibited proteolytic cleavage of the PTH1R
164 ECD, suggesting that the main cleavage site is located in this region. $PTH1R^{72-79A}$ exhibited
165 incomplete inhibition of cleavage, suggesting another, less susceptible cleavage site or an
166 incomplete masking of the cleavage site around residues 56-63.

167 To corroborate these findings, we determined the amino acid sequence of the N-terminus of
168 the cleaved 80 kDa fragment of PTH1R. PTH1R was purified from stably expressing Flp-In
169 CHO cells via a C-terminal Strep2 tag. 50 µg of purified protein were blotted onto PVDF
170 membrane and stained with Coomassie blue. A band corresponding to the cleaved PTH1R
171 fragment was excised and analyzed by Edman degradation (Fig. 3A). Three different N-
172 termini were identified, located at positions Ser^{65}, Ser^{73} and Lys^{80} in the ECD of PTH1R (Fig.
173 3B). Finally, the complete ECD of PTH1R (residues 23-177) was subjected to a
174 computational cleavage site search using positional weight matrices (PWM) for 11 matrix
175 metalloproteinases (MMPs) (30). This procedure revealed a total of 19 putative cleavage sites
176 located between residues 30 to 173. However, only cleavage site Ser^{61}↓Ile^{62} was common to
177 all 11 MMPs and exhibited the highest PWM scores among all other predicted cleavage sites
178 (Table 1). Taken together, these findings support the results of the alanine scan, suggesting
179 that cleavage occurs at Ser^{61}↓Ile^{62} of PTH1R.

180 To test whether ECD cleavage affected receptor function, we assessed activation of the two
181 canonical signaling pathways of PTH1R $G\alpha_s$ (cyclic AMP, cAMP) and $G\alpha_q$ (inositol
182 phosphates, IP) by wild type PTH1R, by the fully cleavage-deficient mutant $PTH1R^{56\text{-}63A}$, and
183 by the partially cleaved mutant $PTH1R^{72\text{-}79A}$. All measurements were performed in stably
184 expressing CHO cells that had been matched for equal receptor expression levels. Compared
185 to wild-type PTH1R, maximal PTH-induced generation of cAMP was reduced by 37% for
186 $PTH1R^{56\text{-}63A}$, whereas no change was observed for $PTH1R^{72\text{-}76A}$ (Fig. 4A, Table 2). In
187 contrast, PTH-induced generation of $[^3H]$IP was increased by 35% for $PTH1R^{56\text{-}63A}$, whereas
188 no change was observed for $PTH1R^{72\text{-}79A}$ (Fig. 4B, Table 2). In summary, these findings
189 suggest, that full cleavage of the ECD of PTH1R leads to decreased efficacy of PTH(1-34) in
190 $G\alpha_q$ signaling and increased efficacy in $G\alpha_s$ signaling. $PTH1R^{72\text{-}79A}$ did not differ from wild-
191 type PTH1R, which may be explained by the fact that the majority of $PTH1R^{72\text{-}79A}$ was still
192 proteolytically processed (c.f. Fig. 3B). Thus, cleavage appears to directly modulate the
193 signaling bias of PTH1R.

194 Discussion

195 Previously, we have reported the ECD of PTH1R is subject to cleavage by
196 metalloproteinases. PTH1R cleavage is a constitutive phenomenon and is inhibited by
197 receptor activation (26). In the present study we aimed to characterize the role of proteolytic
198 processing of the extracellular domain, and we provide evidence for the exact location of the
199 cleavage site as well as for a modulation of signaling properties upon cleavage. N-terminal
200 sequencing of the 80 kDa receptor core (remaining after shedding of the cleaved N-terminal
201 fragment) revealed three nearby cleavage sites ($Glu^{64}\downarrow Ser^{65}$, $Ala^{72}\downarrow Ser^{73}$ and $Arg^{79}\downarrow Lys^{80}$).
202 However, computational analysis using cleavage patterns of 11 MMPs suggested a putative
203 cleavage site at $Ser^{61}\downarrow Ile^{62}$ which was located 3 amino acids upstream of the first free N-
204 terminus identified by microsequencing. A systematic alanine scan within this region of the
205 ECD showed, that only $PTH1R^{56\text{-}63A}$ was completely resistant to proteolysis, while mutation
206 of residues 64-71 to alanine did not prevent proteolysis, further supporting the proximal site at
207 residue 61. Only a fraction of $PTH1R^{72\text{-}79A}$ remained intact whereas the majority of receptor
208 was found as the cleaved 80 kDa form. This may suggest, that the alanine mutations at
209 residues 72-79 mask the cleavage site around residues 56-63 to some extent or may hamper
210 protease interaction resulting in incomplete protease cleavage. We thus propose that
211 $Ser^{61}\downarrow Ile^{62}$ is the primary cleavage site while the free N-termini observed in Edman
212 degradation at Ser^{65}, Ser^{73} and Lys^{80} are most likely the result of limited exopeptidase action

213 following endopeptidase cleavage. Ser^{61} is located within the first residues of a large loop
214 connecting the top layer formed by α1-helix with the first β-strand of the middle layer of the
215 α-β-β-α fold of PTH1R ECD. Notably, residues 61-104 were not resolved in any structure of
216 PTH1R-ECD or full length PTH1R suggesting high flexibility in this region (4,7,31).
217 Considering the orientation of the ECD in the full-length structures, Ser^{61} would be located at
218 the distal part of the receptor facing away from the membrane and, thus, may be well
219 accessible for extracellular proteases (Fig 1).

220 Processing by MMPs and other metalloproteinases has been described previously for a limited
221 number of other GPCRs, i.e. for beta-adrenergic receptor 1 (32), endothelin B receptor
222 (33,34), thyrotropin receptor (35,36), protease-activated receptor 1 (PAR-1) (37,38), GPR124
223 (39) and more recently for GPR37 (40,41). Apart from PAR-1 and the adhesion family
224 receptor GPR124, where protease cleavage unmasks the endogenous ligand resulting in
225 receptor activation, a functional consequence of protease cleavage has not been explicitly
226 reported. To our surprise, proteolytic cleavage of the PTH1R ECD directly affected receptor
227 signaling. In contrast to wild-type receptor, the cleavage-deficient mutant $PTH1R^{56\text{-}63A}$
228 exhibited reduced cAMP and increased IP responses to PTH stimulation. Protease cleavage
229 thus enhanced coupling efficacy of the receptor to the G_s pathway, while reducing G_q-
230 coupling at the same time, resulting in a signaling bias. Biased signaling is defined as ligands
231 giving different degrees of activation in separate signaling pathways on the same receptor.
232 Besides binding of ligands to allosteric sites on the receptor that stabilize distinct active
233 receptor conformations, interaction of a receptor with intracellular adaptor proteins and
234 subcellular receptor sequestration have been reported to affect signaling bias (42-44). For the
235 PTH1R, several ligands and intracellular adaptors which direct signaling specificity to G_s, G_q
236 or G protein-independent pathways have been described (17,22,24,29,45-48). All of these
237 PTH/PTHrP derivatives carry modifications at the N-terminal part, which directly interacts
238 with the transmembrane domain of the receptor, suggesting that signaling specificity is
239 mediated by direct conformational stabilization of the receptor core. Our findings now
240 indicate that the ECD, which accommodates the C-terminal part of PTH and which is
241 commonly believed to only serve as an "affinity trap" for the ligand, can also affect signaling
242 specificity of the receptor.

243 There is growing evidence, that extracellular regions of GPCRs play important roles in fine-
244 tuning receptor activity and signaling selectivity. Apart from PARs and adhesion receptors,
245 where the buried orthosteric ligand is proteolytically released from the receptor's N-terminus,

246 extracellular loops play an important role in modulating the function of several class A and
247 class B receptors (49). More importantly, calcium-mediated interaction of extracellular loop 1
248 and PTH has been shown to allosterically modulate PTH1R activity (50-52). Recent studies
249 on glucagon receptor suggest that the ECD itself may act as an allosteric inhibitor by
250 interaction of α1-helix of the ECD with extracellular loop 3 of the receptor core (53).
251 Moreover, recent cryo-EM structures of active-state class B GPCRs including PTH1R reveal
252 a high degree of conformational flexibility of the ECD (31,54,55), and it has been proposed
253 that the dynamic motion of the ECD may contribute to biased agonism of class B GPCR
254 ligands (56,57). In line with that, an antibody primarily binding to α1-helix of the ECD has
255 been shown to modulate β-arrestin signaling of PTH1R (58) suggesting that perturbation of
256 the ECD orientation or ECD conformation may alter receptor signaling. Proteolytic cleavage
257 at Ser^{61} is expected to result in increased conformational flexibility of the α1-helix of PTH1R
258 ECD as the helix remains tethered to the receptor only through a disulfide bond between
259 Cys^{48} and Cys^{117} (26) (Fig. 5). As a consequence, especially the N-terminal part of α1-helix
260 which is facing towards the TMD in the ligand-bound receptor (Fig. 1) (7) may gain
261 additional flexibility. Notably, within this region residues 32-41 make important contacts to
262 PTH including the flexible central region of the peptide (4,7) (Fig 5.). This region was shown
263 to be critical for initiating the two-step binding mechanism of PTH (59). Thus, it may well be
264 conceivable that alterations in the flexibility and orientation of α1-helix of PTH1R ECD can
265 allosterically affect receptor signaling. Whether these effects are mediated by an altered
266 interaction of the ECD with the transmembrane core, by a rearrangement of the ligand in the
267 binding pocket, or involve interaction of additional proteins such as RAMPs (receptor
268 activity-modifying proteins) with PTH1R (60) needs to be studied.

269 In summary, we have mapped the cleavage site within the ECD of PTH1R and demonstrate
270 for the first time, to our knowledge, that protease cleavage of the ECD of a GPCR modulates
271 G protein signaling specificity.

Conflict of Interest

The authors declare that the research was conducted in the absence of any commercial or financial relationships that could be construed as a potential conflict of interest.

Author Contributions

CK and MJL conceived the study; CK designed experiments; CK and LH performed experiments; CK, LH and MJL analyzed data; CK wrote the manuscript, all authors provided edits and comments.

Funding

These studies were supported by grants from the Deutsche Forschungsgemeinschaft (SFB487) and the European Research Council (Advanced Grant TOPAS, No. 232944) to MJL.

Acknowledgments

We thank Michaela Hoffmann, Annette Hannawacker, Alexandra Bohl and Monika Frank for technical assistance. Moreover, we thank Dr. Thomas Pohl (Wita GmbH, Berlin) for support with N-terminal microsequencing.

287 **References**

288 1. Jüppner H, Abou-Samra AB, Uneno S, Gu WX, Potts JT, Segre GV. The parathyroid
289 hormone-like peptide associated with humoral hypercalcemia of malignancy and
290 parathyroid hormone bind to the same receptor on the plasma membrane of ROS 17/2.8
291 cells. *J Biol Chem* (1988) **263**:8557–8560.

292 2. Fredriksson R, Lagerström MC, Lundin L-G, Schiöth HB. The G-protein-coupled
293 receptors in the human genome form five main families. Phylogenetic analysis,
294 paralogon groups, and fingerprints. *Mol Pharmacol* (2003) **63**:1256–1272.
295 doi:10.1124/mol.63.6.1256

296 3. Lagerström MC, Schiöth HB. Structural diversity of G protein-coupled receptors and
297 significance for drug discovery. *Nat Rev Drug Discov* (2008) **7**:339–357.
298 doi:10.1038/nrd2518

299 4. Pioszak AA, Xu HE. Molecular recognition of parathyroid hormone by its G protein-
300 coupled receptor. *Proc Natl Acad Sci U S A* (2008) **105**:5034–5039.
301 doi:10.1073/pnas.0801027105

302 5. Grauschopf U, Lilie H, Honold K, Wozny M, Reusch D, Esswein A, Schäfer W,
303 Rücknagel KP, Rudolph R. The N-terminal fragment of human parathyroid hormone
304 receptor 1 constitutes a hormone binding domain and reveals a distinct disulfide
305 pattern. *Biochemistry* (2000) **39**:8878–8887.

306 6. Karpf DB, Arnaud CD, Bambino T, Duffy D, King KL, Winer J, Nissenson RA.
307 Structural properties of the renal parathyroid hormone receptor: hydrodynamic analysis
308 and protease sensitivity. *Endocrinology* (1988) **123**:2611–2620.

309 7. Ehrenmann J, Schöppe J, Klenk C, Rappas M, Kummer L, Doré AS, Plückthun A.
310 High-resolution crystal structure of parathyroid hormone 1 receptor in complex with a
311 peptide agonist. *Nat Struct Mol Biol* (2018) **25**:1086–1092. doi:10.1038/s41594-018-
312 0151-4

313 8. Castro M, Nikolaev VO, Palm D, Lohse MJ, Vilardaga J-P. Turn-on switch in
314 parathyroid hormone receptor by a two-step parathyroid hormone binding mechanism.
315 *Proc Natl Acad Sci U S A* (2005) **102**:16084–16089. doi:10.1073/pnas.0503942102

316 9. Gensure RC, Gardella TJ, Jüppner H. Parathyroid hormone and parathyroid hormone-
317 related peptide, and their receptors. *Biochem Biophys Res Commun* (2005) **328**:666–
318 678. doi:10.1016/j.bbrc.2004.11.069

319 10. Friedman PA. PTH revisited. *Kidney Int Suppl* (2004)S13–S19. doi:10.1111/j.1523-
320 1755.2004.09103.x

321 11. Jüppner H, Abou-Samra AB, Freeman M, Kong XF, Schipani E, Richards J,
322 Kolakowski LF, Hock J, Potts JT, Kronenberg HM. A G protein-linked receptor for
323 parathyroid hormone and parathyroid hormone-related peptide. *Science* (1991)
324 **254**:1024–1026.

325 12. Vilardaga J-P, Romero G, Friedman PA, Gardella TJ. Molecular basis of parathyroid
326 hormone receptor signaling and trafficking: a family B GPCR paradigm. *Cell Mol Life*
327 *Sci* (2011) **68**:1–13. doi:10.1007/s00018-010-0465-9

328 13. Cole JA. Parathyroid hormone activates mitogen-activated protein kinase in opossum
329 kidney cells. *Endocrinology* (1999) **140**:5771–5779. doi:10.1210/endo.140.12.7173

330 14. Mahon MJ, Bonacci TM, Divieti P, Smrcka AV. A docking site for G protein βγ
331 subunits on the parathyroid hormone 1 receptor supports signaling through multiple
332 pathways. *Mol Endocrinol* (2006) **20**:136–146. doi:10.1210/me.2005-0169

333 15. Singh ATK, Gilchrist A, Voyno-Yasenetskaya T, Radeff-Huang JM, Stern PH. G
334 alpha12/G alpha13 subunits of heterotrimeric G proteins mediate parathyroid hormone
335 activation of phospholipase D in UMR-106 osteoblastic cells. *Endocrinology* (2005)
336 **146**:2171–2175. doi:10.1210/en.2004-1283

337 16. Malecz N, Bambino T, Bencsik M, Nissenson RA. Identification of phosphorylation
338 sites in the G protein-coupled receptor for parathyroid hormone. Receptor
339 phosphorylation is not required for agonist-induced internalization. *Mol Endocrinol*
340 (1998) **12**:1846–1856.

341 17. Gesty-Palmer D, Chen M, Reiter E, Ahn S, Nelson CD, Wang S, Eckhardt AE, Cowan
342 CL, Spurney RF, Luttrell LM, et al. Distinct beta-arrestin- and G protein-dependent
343 pathways for parathyroid hormone receptor-stimulated ERK1/2 activation. *J Biol Chem*
344 (2006) **281**:10856–10864. doi:10.1074/jbc.M513380200

345 18. Schwindinger WF, Fredericks J, Watkins L, Robinson H, Bathon JM, Pines M, Suva
346 LJ, Levine MA. Coupling of the PTH/PTHrP receptor to multiple G-proteins. Direct
347 demonstration of receptor activation of Gs, Gq/11, and Gi(1) by [alpha-32P]GTP-
348 gamma-azidoanilide photoaffinity labeling. *Endocrine* (1998) **8**:201–209.
349 doi:10.1385/ENDO:8:2:201

350 19. Jilka RL. Molecular and cellular mechanisms of the anabolic effect of intermittent
351 PTH. *Bone* (2007) **40**:1434–1446. doi:10.1016/j.bone.2007.03.017

352 20. Lee M, Partridge NC. Parathyroid hormone signaling in bone and kidney. *Curr Opin*
353 *Nephrol Hypertens* (2009) **18**:298–302. doi:10.1097/MNH.0b013e32832c2264

354 21. Whitfield JF, Morley P, Willick GE, Ross V, Barbier JR, Isaacs RJ, Ohannessian-Barry
355 L. Stimulation of the growth of femoral trabecular bone in ovariectomized rats by the
356 novel parathyroid hormone fragment, hPTH-(1-31)NH2 (Ostabolin). *Calcif Tissue Int*
357 (1996) **58**:81–87.

358 22. Yang D, Singh R, Divieti P, Guo J, Bouxsein ML, Bringhurst FR. Contributions of
359 parathyroid hormone (PTH)/PTH-related peptide receptor signaling pathways to the
360 anabolic effect of PTH on bone. *Bone* (2007) **40**:1453–1461.
361 doi:10.1016/j.bone.2007.02.001

362 23. Hilliker S, Wergedal JE, Gruber HE, Bettica P, Baylink DJ. Truncation of the amino
363 terminus of PTH alters its anabolic activity on bone in vivo. *Bone* (1996) **19**:469–477.

364 24. Gesty-Palmer D, Flannery P, Yuan L, Corsino L, Spurney R, Lefkowitz RJ, Luttrell
365 LM. A beta-arrestin-biased agonist of the parathyroid hormone receptor (PTH1R)
366 promotes bone formation independent of G protein activation. *Sci Transl Med* (2009)
367 **1**:1ra1. doi:10.1126/scitranslmed.3000071

368 25. Potts JT. Parathyroid hormone: past and present. *J Endocrinol* (2005) **187**:311–325.

369 doi:10.1677/joe.1.06057

370 26. Klenk C, Schulz S, Calebiro D, Lohse MJ. Agonist-regulated cleavage of the
371 extracellular domain of parathyroid hormone receptor type 1. *J Biol Chem* (2010)
372 **285**:8665–8674. doi:10.1074/jbc.M109.058685

373 27. Lupp A, Klenk C, Röcken C, Evert M, Mawrin C, Schulz S. Immunohistochemical
374 identification of the PTHR1 parathyroid hormone receptor in normal and neoplastic
375 human tissues. *Eur J Endocrinol* (2010) **162**:979–986. doi:10.1530/EJE-09-0821

376 28. Klenk C, Vetter T, Zürn A, Vilardaga J-P, Friedman PA, Wang B, Lohse MJ.
377 Formation of a ternary complex among NHERF1, beta-arrestin, and parathyroid
378 hormone receptor. *J Biol Chem* (2010) **285**:30355–30362.
379 doi:10.1074/jbc.M110.114900

380 29. Emami-Nemini A, Gohla A, Urlaub H, Lohse MJ, Klenk C. The guanine nucleotide
381 exchange factor Vav2 is a negative regulator of parathyroid hormone receptor/Gq
382 signaling. *Mol Pharmacol* (2012) **82**:217–225. doi:10.1124/mol.112.078824

383 30. Kumar S, Ratnikov BI, Kazanov MD, Smith JW, Cieplak P. CleavPredict: A Platform
384 for Reasoning about Matrix Metalloproteinases Proteolytic Events. *PLoS ONE* (2015)
385 **10**:e0127877. doi:10.1371/journal.pone.0127877

386 31. Zhao L-H, Ma S, Sutkeviciute I, Shen D-D, Zhou XE, de Waal PW, Li C-Y, Kang Y,
387 Clark LJ, Jean-Alphonse FG, et al. Structure and dynamics of the active human
388 parathyroid hormone receptor-1. *Science* (2019) **364**:148–153.
389 doi:10.1126/science.aav7942

390 32. Hakalahti AE, Vierimaa MM, Lilja MK, Kumpula E-P, Tuusa JT, Petäjä-Repo UE.
391 Human beta1-Adrenergic Receptor Is Subject to Constitutive and Regulated N-terminal
392 Cleavage. *J Biol Chem* (2010) **285**:28850–28861. doi:10.1074/jbc.M110.149989

393 33. Kozuka M, Ito T, Hirose S, Lodhi KM, Hagiwara H. Purification and characterization
394 of bovine lung endothelin receptor. *J Biol Chem* (1991) **266**:16892–16896.

395 34. Grantcharova E, Furkert J, Reusch HP, Krell H-W, Papsdorf G, Beyermann M,
396 Schulein R, Rosenthal W, Oksche A. The extracellular N terminus of the endothelin B
397 (ETB) receptor is cleaved by a metalloprotease in an agonist-dependent process. *J Biol*
398 *Chem* (2002) **277**:43933–43941. doi:10.1074/jbc.M208407200

399 35. Couet J, Sar S, Jolivet A, Hai MT, Milgrom E, Misrahi M. Shedding of human
400 thyrotropin receptor ectodomain. Involvement of a matrix metalloprotease. *J Biol*
401 *Chem* (1996) **271**:4545–4552.

402 36. Kaczur V, Puskas LG, Nagy ZU, Miled N, Rebai A, Juhasz F, Kupihar Z, Zvara A,
403 Hackler L, Farid NR. Cleavage of the human thyrotropin receptor by ADAM10 is
404 regulated by thyrotropin. *J Mol Recognit* (2007) **20**:392–404. doi:10.1002/jmr.851

405 37. Boire A, Covic L, Agarwal A, Jacques S, Sherifi S, Kuliopulos A. PAR1 is a matrix
406 metalloprotease-1 receptor that promotes invasion and tumorigenesis of breast cancer
407 cells. *Cell* (2005) **120**:303–313. doi:10.1016/j.cell.2004.12.018

408 38. Ludeman MJ, Zheng YW, Ishii K, Coughlin SR. Regulated shedding of PAR1 N-

409 terminal exodomain from endothelial cells. *J Biol Chem* (2004) **279**:18592–18599.
410 doi:10.1074/jbc.M310836200

411 39. Vallon M, Essler M. Proteolytically processed soluble tumor endothelial marker (TEM)
412 5 mediates endothelial cell survival during angiogenesis by linking integrin
413 alpha(v)beta3 to glycosaminoglycans. *J Biol Chem* (2006) **281**:34179–34188.
414 doi:10.1074/jbc.M605291200

415 40. Mattila SO, Tuhkanen HE, Lackman JJ, Konzack A, Morató X, Argerich J, Saftig P,
416 Ciruela F, Petäjä-Repo UE. GPR37 is processed in the N-terminal ectodomain by
417 ADAM10 and furin. *FASEB J* (2021) **35**:e21654. doi:10.1096/fj.202002385RR

418 41. Mattila SO, Tuusa JT, Petäjä-Repo UE. The Parkinson's-disease-associated receptor
419 GPR37 undergoes metalloproteinase-mediated N-terminal cleavage and ectodomain
420 shedding. *J Cell Sci* (2016) **129**:1366–1377. doi:10.1242/jcs.176115

421 42. Luttrell LM, Maudsley S, Bohn LM. Fulfilling the Promise of "Biased" G Protein-
422 Coupled Receptor Agonism. *Mol Pharmacol* (2015) **88**:579–588.
423 doi:10.1124/mol.115.099630

424 43. Kenakin TP. New concepts in pharmacological efficacy at 7TM receptors: IUPHAR
425 review 2. *Br J Pharmacol* (2013) **168**:554–575. doi:10.1111/j.1476-5381.2012.02223.x

426 44. Onaran HO, Rajagopal S, Costa T. What is biased efficacy? Defining the relationship
427 between intrinsic efficacy and free energy coupling. *Trends Pharmacol Sci* (2014)
428 **35**:639–647. doi:10.1016/j.tips.2014.09.010

429 45. Bisello A, Chorev M, Rosenblatt M, Monticelli L, Mierke DF, Ferrari SL. Selective
430 ligand-induced stabilization of active and desensitized parathyroid hormone type 1
431 receptor conformations. *J Biol Chem* (2002) **277**:38524–38530.
432 doi:10.1074/jbc.M202544200

433 46. Takasu H, Gardella TJ, Luck MD, Potts JT, Bringhurst FR. Amino-terminal
434 modifications of human parathyroid hormone (PTH) selectively alter phospholipase C
435 signaling via the type 1 PTH receptor: implications for design of signal-specific PTH
436 ligands. *Biochemistry* (1999) **38**:13453–13460.

437 47. Jouishomme H, Whitfield JF, Chakravarthy B, Durkin JP, Gagnon L, Isaacs RJ,
438 Maclean S, Neugebauer W, Willick G, Rixon RH. The protein kinase-C activation
439 domain of the parathyroid hormone. *Endocrinology* (1992) **130**:53–60.
440 doi:10.1210/endo.130.1.1727720

441 48. Azarani A, Goltzman D, Orlowski J. Structurally diverse N-terminal peptides of
442 parathyroid hormone (PTH) and PTH-related peptide (PTHRP) inhibit the Na+/H+
443 exchanger NHE3 isoform by binding to the PTH/PTHRP receptor type I and activating
444 distinct signaling pathways. *J Biol Chem* (1996) **271**:14931–14936.

445 49. Wheatley M, Wootten D, Conner MT, Simms J, Kendrick R, Logan RT, Poyner DR,
446 Barwell J. Lifting the lid on GPCRs: the role of extracellular loops. *Br J Pharmacol*
447 (2012) **165**:1688–1703. doi:10.1111/j.1476-5381.2011.01629.x

448 50. White AD, Fang F, Jean-Alphonse FG, Clark LJ, An H-J, Liu H, Zhao Y, Reynolds
449 SL, Lee S, Xiao K, et al. Ca2+ allostery in PTH-receptor signaling. *Proc Natl Acad Sci*

450 *U S A* (2019) **116**:3294–3299. doi:10.1073/pnas.1814670116

451 51. Li M, Li M, Guo J. Molecular Mechanism of Ca2+ in the Allosteric Regulation of
452 Human Parathyroid Hormone Receptor-1. *J Chem Inf Model* (2021)
453 doi:10.1021/acs.jcim.1c00471

454 52. Mitra N, Liu Y, Liu J, Serebryany E, Mooney V, Devree BT, Sunahara RK, Yan ECY.
455 Calcium-dependent ligand binding and G-protein signaling of family B GPCR
456 parathyroid hormone 1 receptor purified in nanodiscs. *ACS Chem Biol* (2013) **8**:617–
457 625. doi:10.1021/cb300466n

458 53. Koth CM, Murray JM, Mukund S, Madjidi A, Minn A, Clarke HJ, Wong T, Chiang V,
459 Luis E, Estevez A, et al. Molecular basis for negative regulation of the glucagon
460 receptor. *Proc Natl Acad Sci U S A* (2012) **109**:14393–14398.
461 doi:10.1073/pnas.1206734109

462 54. Liang Y-L, Khoshouei M, Deganutti G, Glukhova A, Koole C, Peat TS, Radjainia M,
463 Plitzko JM, Baumeister W, Miller LJ, et al. Cryo-EM structure of the active, Gs-protein
464 complexed, human CGRP receptor. *Nature* (2018) **561**:492–497. doi:10.1038/s41586-
465 018-0535-y

466 55. Dal Maso E, Glukhova A, Zhu Y, García-Nafría J, Tate CG, Atanasio S, Reynolds CA,
467 Ramírez-Aportela E, Carazo J-M, Hick CA, et al. The Molecular Control of Calcitonin
468 Receptor Signaling. *ACS Pharmacology & Translational Science* (2019) **2**:31–51.
469 doi:10.1021/acsptsci.8b00056

470 56. Liang Y-L, Khoshouei M, Glukhova A, Furness SGB, Zhao P, Clydesdale L, Koole C,
471 Truong TT, Thal DM, Lei S, et al. Phase-plate cryo-EM structure of a biased agonist-
472 bound human GLP-1 receptor–Gs complex. *Nature* (2018) **68**:954.
473 doi:10.1002/jcc.20084

474 57. Lei S, Clydesdale L, Dai A, Cai X, Feng Y, Yang D, Liang Y-L, Koole C, Zhao P,
475 Coudrat T, et al. Two distinct domains of the glucagon-like peptide-1 receptor control
476 peptide-mediated biased agonism. *J Biol Chem* (2018) **293**:9370–9387.
477 doi:10.1074/jbc.RA118.003278

478 58. Sarkar K, Joedicke L, Westwood M, Burnley R, Wright M, McMillan D, Byrne B.
479 Modulation of PTH1R signaling by an ECD binding antibody results in inhibition of β-
480 arrestin 2 coupling. *Sci Rep* (2019) **9**:14432. doi:10.1038/s41598-019-51016-z

481 59. Clark LJ, Clark LJ, Krieger J, Krieger J, White AD, White AD, Bondarenko V,
482 Bondarenko V, Lei S, Lei S, et al. Allosteric interactions in the parathyroid hormone
483 GPCR–arrestin complex formation. *Nat Chem Biol* (2020) **42**:946.
484 doi:10.1007/s13361-011-0261-2

485 60. Christopoulos A, Christopoulos G, Morfis M, Udawela M, Laburthe M, Couvineau A,
486 Kuwasako K, Tilakaratne N, Sexton PM. Novel receptor partners and function of
487 receptor activity-modifying proteins. *J Biol Chem* (2003) **278**:3293–3297.
488 doi:10.1074/jbc.C200629200

489 61. Schechter I, Berger A. On the size of the active site in proteases. I. Papain. *Biochem*
490 *Biophys Res Commun* (1967) **27**:157–162. doi:10.1016/j.bbrc.2012.08.015

491 # Tables

492 **Table 1 – Computational cleavage site prediction of PTH1R ECD.** The sequence of the
493 mature PTH1R ECD (amino acids 23-177) was analyzed for MMP cleavage sites with
494 CleavPredict (30) using position weight matrices for 11 MMPs (MMP-2, MMP-3, MMP-8,
495 MMP-9, MMP-13, MMP-14, MMP-15, MMP-16, MMP-17, MMP-24, MMP-25). For each
496 cleavage site, the residue number of P1, the sequence corresponding to P5-P5' (numbering
497 according to Schechter and Berger (61)) and the position weight matrix score (PWM score)
498 for each MMP subtype are given.

P1 position	residues (P5-P5')	MMP										
		2	3	8	9	10	14	15	16	17	24	25
30	VDADD↓VMTKE											1.32
37	TKEEQ↓IFLLH											0.19
40	EQIFL↓LHRAQ		3.46			2.19				3.43		1.50
46	HRAQA↓QCEKR									2.37		1.71
51	QCEKR↓LKEVL											
61	QRPAS↓IMESD	6.75	8.76	6.13	5.72	8.26	7.60	5.37	7.00	3.42	7.88	5.82
80	GKPRK↓DKASG	1.36										
86	KASGK↓LYPES			1.63				1.31		2.44		4.71
100	EAPTG↓SRYRG				2.52							
102	PTGSR↓YRGRP			1.90								
114	PEWDH↓ILCWP							2.62				
125	GAPGE↓VVAVP	3.56	3.14	2.03								0.21
134	PCPDY↓IYDFN			2.48		1.64		5.02				4.48
137	DYIYD↓FNHKG			2.06								
144	HKGHA↓YRRCD			2.67							0.81	
155	NGSWE↓LVPGH			5.18						2.47		4.00
160	LVPGH↓NRTWA	2.05					1.74	2.03	1.35			
166	RTWAN↓YSECV						1.97		2.16			
173	ECVKF↓LTNET			3.15	6.44		1.30		2.98	3.50		4.39

499

500

501 **Table 2 – Effects of ECD cleavage on cAMP generation and IP accumulation.** PTH-
502 induced E_{max} values for cAMP and IP generation of $PTH1R^{56-63A}$ or $PTH1R^{72-79A.}$ were
503 compared against that of PTH1R using unpaired t tests. Data summarize results of 3-5
504 independent experiments.

	Difference vs. PTH1R, cAMP (%)			Difference vs. PTH1R, [^{3}H] IP (%)		
	Mean ± SEM	95% C.I.	*p*	Mean ± SEM	95% C.I.	*p*
$PTH1R^{56-63A}$	-37.3 ± 5.9	-52.7 to -21.9	0.0015	35.3 ± 10.7	10.6 to 60.1	0.011
$PTH1R^{72-79A}$	-1.9 ± 1.3	-5.3 to 1.5	0.21	-5.6 ± 19.4	-48.8 to 37.6	0.78

C.I., confidence interval

505

506

507 **Figures**

508

509 **Figure 1 – Topology of PTH1R.** Structure of the human PTH1R (teal) in complex with a
510 PTH analog (orange) (PDB ID: 6FJ3). Unstructured residues 60-106 of ECD loop 1 are
511 shown as a dashed line.

512

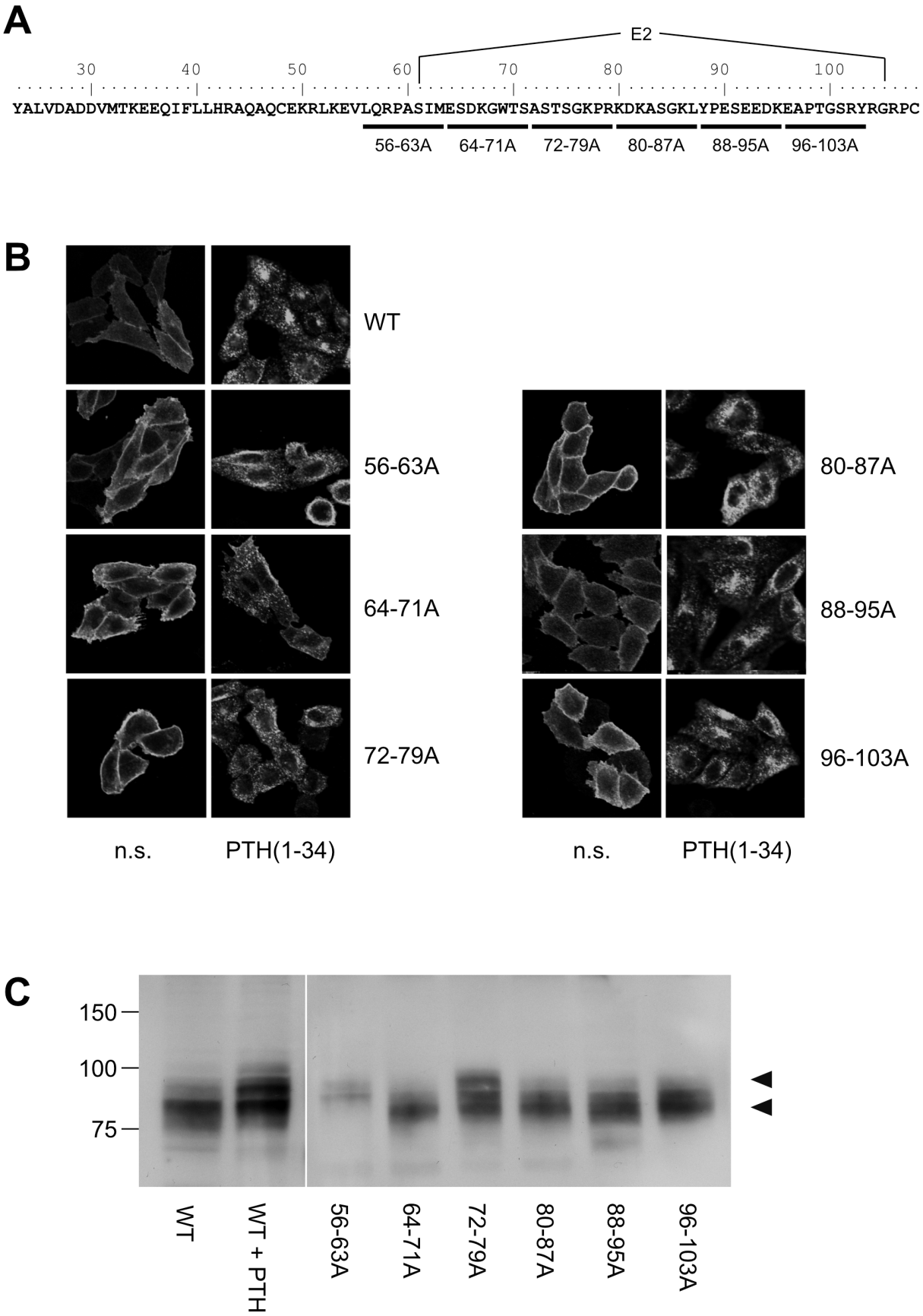
A
E2
30 40 50 60 70 80 90 100
YALVDADDVMTKEEQIFLLHRAQAQCEKRLKEVLQRPASIMESDKGWTSASTSGKPRKDKASGKLYPESEEDKEAPTGSRYRGRPC
56-63A
64-71A
72-79A
80-87A
88-95A
96-103A
B
WT
56-63A
64-71A
72-79A
80-87A
88-95A
96-103A
n.s.
PTH(1-34)
n.s.
PTH(1-34)
C
150
100
75
WT
WT + PTH
56-63A
64-71A
72-79A
80-87A
88-95A
96-103A

513

514 **Figure 2 – Mapping of the protease cleavage site of PTH1R ECD by alanine scan. (A)**
515 Amino acid sequence of the N-terminal part of PTH1R ECD. Stretches of 8 amino acids that
516 were replaced by alanine residues are indicated by horizontal bars. Exon E2 is marked above
517 the sequence. **(B)** CHO cells stably expressing PTHR variants were treated with 100 nM
518 PTH(1-34) for 30 min or left untreated. Subsequently, cells were fixed, permeabilized, and
519 stained with rabbit anti-PTH1R antibody followed by Cy2-labeled anti-rabbit antibody. PTHR
520 was visualized by confocal microscopy. **(C)** CHO cells stably expressing PTHR variants were
521 lysed, and PTH1R was monitored by reducing SDS-PAGE and Western blotting. Cells were
522 treated with 100 nM PTH(1-34) for 12 h prior to cell lysis where indicated. Arrowheads
523 depict the cleaved (MW ~80 kDa) and the uncleaved (MW ~90 kDa) PTH1R band.

524

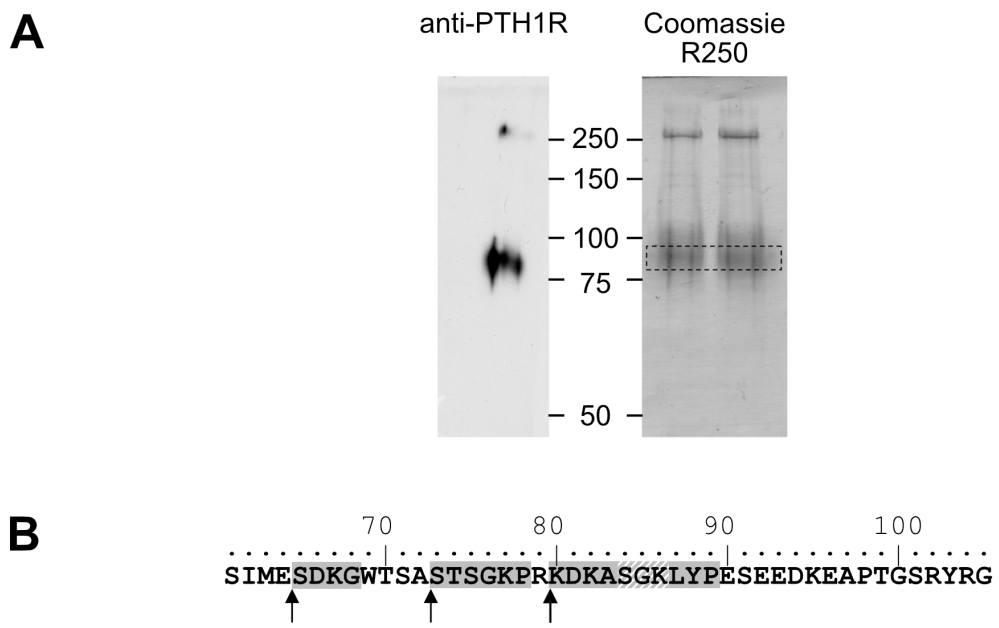

525

526 **Figure 3 – Mapping of the protease cleavage site of PTH1R ECD by N-terminal**
527 **sequencing. (A)** Human PTH1R with C-terminal Strep2-tag was purified from stably
528 expressing CHO cells by two-step affinity purification. A fraction of the purified receptor was
529 subjected to Western blot and probed with anti-PTH1R antibodies (left panel). The remaining
530 purified receptor protein (~50 µg) was transferred on PVDF membranes and stained with
531 Coomassie blue R250. The band corresponding to PTH1R was cut out and subjected to
532 microsequencing (right panel, dashed box). **(B)** Sequence of exon E2 (amino acids 61-105).
533 Sequences obtained from microsequencing are shaded gray. The position of the N-terminal
534 amino acid is marked by an arrow. Residues 84-86 were not resolved in the Edman
535 degradation.

536

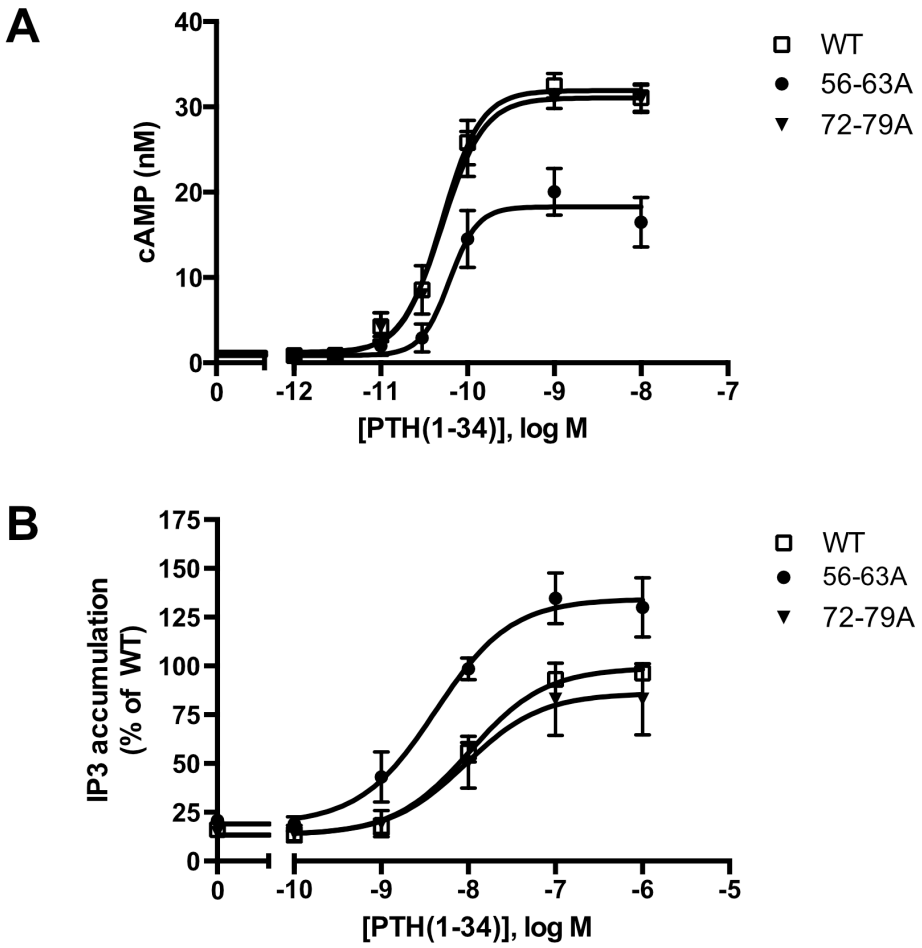

537

538 **Figure 4 – Protease cleavage changes the signaling specificity of PTH1R from $G\alpha_q$ and**
539 **$G\alpha_s$. (A)** Flp-In CHO cells stably expressing PTH1R, $PTH1R^{56\text{-}63A}$ or $PTH1R^{72\text{-}79A}$ were
540 stimulated for 20 min with PTH(1-34) at the indicated concentrations, and cAMP levels were
541 quantified with a radioimmunoassay. The means ± S.E.M. of five independent experiments
542 are shown. **(B)** Flp-In CHO cells stably expressing PTH1R, $PTH1R^{56\text{-}63A}$ or $PTH1R^{72\text{-}79A}$
543 were incubated with [*myo*-2-^{3}H(N)]inositol and 0.2% fetal calf serum for 16 h. Cells were
544 stimulated for 60 min with the indicated concentrations of PTH, and [^{3}H]IP_3 levels were
545 quantified in a scintillation counter after chromatographic separation. Data represent the
546 means ± S.E.M. of five individual experiments.

547

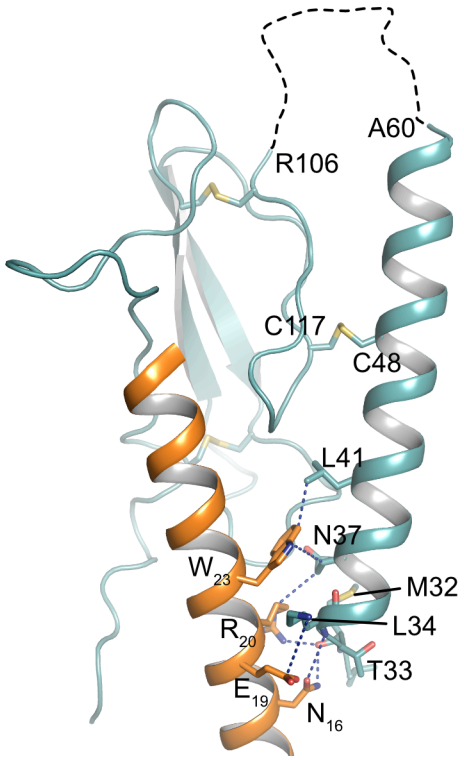

548

549 **Figure 5 – Interface between PTH and α1-helix of PTH1R ECD.** Crystal structure of the
550 PTH1R ECD (teal) in complex with PTH (orange) (PDB ID: 6FJ3). Residues forming the
551 interface are shown as stick and contacts are indicated as blue dashed lines. The unstructured
552 loop 1 of the ECD is shown as black dashed line.